

# A large age for the pulsar B1757–24 from an upper limit on its proper motion

B. M. Gaensler<sup>\*‡</sup> and D. A. Frail<sup>†</sup>

<sup>\*</sup> Center for Space Research, Massachusetts Institute of Technology, Cambridge, MA 02139, USA

<sup>‡</sup> Hubble Fellow

<sup>†</sup> National Radio Astronomy Observatory, P.O. Box 0, Socorro, NM 87801, USA

---

The “characteristic age”<sup>1</sup> of a pulsar usually is considered to approximate its true age, but this assumption has led to some puzzling results, including the fact that many pulsars with small characteristic ages have no associated supernova remnants.<sup>2,3</sup> The pulsar B1757–24 is located just beyond the edge of a supernova remnant<sup>4–6</sup>; the properties of the system indicate that the pulsar was born at the centre of the remnant, but that it has subsequently overtaken the expanding blast-wave.<sup>5–8</sup> With a characteristic age of 16,000 yr, this implies an expected<sup>8</sup> proper motion by the pulsar of 63–80 milliarcseconds (mas) per year. Here we report observations of the nebula surrounding the pulsar which limit its proper motion to less than 25 mas yr<sup>−1</sup>, implying a minimum age of 39,000 yr. A more detailed analysis argues for a true age as great as 170,000 yr, significantly larger than the characteristic age. From this result and other discrepancies associated with pulsars, we conclude that characteristic ages seriously underestimate the true ages of pulsars.

---

The radio supernova remnant G5.4–1.2 is shown in Fig 1: it has an approximately circular radio morphology of diameter  $\sim 35'$ , but is much brighter and has a significantly flatter spectral index along its western edge.<sup>6,8–10</sup> Approximately  $5'$  beyond this bright western rim is the 125-ms pulsar B1757–24,<sup>4–6</sup> whose rotational frequency,  $\nu$ , and frequency derivative,  $\dot{\nu}$ , can be used to derive a characteristic age,  $\tau \equiv \nu/2\dot{\nu} \approx 16$  kyr. Provided that a pulsar’s initial frequency is much larger than  $\nu$ , that the pulsar slows down by magnetic dipole braking, and that its magnetic dipole moment and moment of inertia do not evolve with time, then  $\tau \approx t_p$ , where  $t_p$  is the pulsar’s true age.<sup>1</sup>

Surrounding the pulsar is the radio nebula G5.27–0.90, whose properties are consistent with it being powered by the pulsar’s relativistic wind.<sup>6,8</sup> G5.27–0.90 has a cometary morphology with a tail pointing back towards the centre of G5.4–1.2, an appearance which strongly suggests that the pulsar is travelling away from the centre of G5.4–1.2 at high velocity. The characteristic age of B1757–24 and its positional offset from the centre of G5.4–1.2 together imply a proper motion of 63–80 milliarcsec yr<sup>−1</sup> (ref. 8). For a distance to the system of 5 kpc,<sup>8</sup> this corresponds to a transverse velocity for the pulsar in the range 1500–1900 km s<sup>−1</sup>, significantly higher than typical pulsar velocities of  $\sim 500$  km s<sup>−1</sup> (refs 11, 12).

To look for this expected proper motion, we have undertaken multi-epoch observations of G5.27–0.90 with the Very Large Array (VLA). Our observations are summarised in Table 1; the two epochs are separated by 6.7 yr. The two data-sets were processed in identical fashion, with results shown in Fig 2. If G5.27–0.90 is associated with the pulsar, then the expected shift of the nebula between these two epochs is 422–526 milliarcsec in a westwardly direction; it is immediately apparent, even by eye, that motion of this magnitude is not observed. The two epochs can be compared

in a more quantitative fashion using the approach described in the legend to Fig 2; we find an offset between the two epochs (in the sense [Epoch 2]–[Epoch 1]) of  $\Delta(\text{RA}) = +39 \pm 41$  milliarcsec and  $\Delta(\text{Dec}) = -9 \pm 34$  milliarcsec, where contributions from both the noise in the images and estimated errors in the phase calibration of the data have been combined in quadrature. We can thus rule out the proper motion which would be expected if  $t_p = \tau$  at the 11–14  $\sigma$  level, independent of the distance adopted to either the pulsar or the SNR.

We now consider various explanations for this surprising discrepancy, and show that the most reasonable explanation is that  $t_p \gg \tau$ . In the following discussion, we only consider proper motion in a westward direction (as implied by the morphology of G5.27–0.90), and adopt a 5- $\sigma$  upper limit on any shift between epochs of 166 milliarcsec, corresponding to a maximum proper motion of 24.8 milliarcsec yr<sup>-1</sup>. For a distance  $d = 5d_5$  kpc and a projected velocity of the nebula  $V_n = 1000v_n$  km s<sup>-1</sup>, this lets us derive an upper limit  $v_n < 0.59d_5$ .

One possible explanation for this unexpectedly low velocity is that the pulsar is moving at  $V_p \sim 1500$  km s<sup>-1</sup>  $\approx 2.5v_n$ , but its associated nebula, sensitive to its surroundings, does not track the ballistic motion of the pulsar on a one-to-one basis. The distance,  $r_w$ , between the pulsar and the head of the bow-shock is determined by pressure balance between the pulsar wind and the ram pressure produced by the pulsar’s motion, such that (ref. 6, 13):

$$\eta \dot{E} / 4\pi r_w^2 c = \frac{4}{9} \rho V_p^2, \quad (1)$$

where  $\rho$  is the mass density of the ambient medium and  $\eta$  is the fraction of the pulsar’s spin-down luminosity,  $\dot{E} \equiv -4\pi^2 I \nu \dot{\nu} = 2.6 \times 10^{36}$  erg s<sup>-1</sup>, which goes into powering its relativistic wind ( $\eta < 1$ ). Using the pulsar’s position as measured in late 1999 (see legend to Fig 2), we find that  $r_w = 0.036d_5$  pc for the second epoch. Assuming that  $v_p = 2.5v_n$  (where  $V_p = 1000v_p$  km s<sup>-1</sup>), we can then infer that  $r_w$  must have decreased by at least 20% between Epochs 1 and 2. A decrease in  $\eta \dot{E}$  by a similar factor can produce this effect. However, comparison of pulsar timing parameters from the time of Epoch 2 (A. G. Lyne, private communication) with those published before Epoch 1 (ref. 5) shows no significant change in  $\dot{E}$ , while a change in  $\eta$  seems unlikely given that changes in the efficiency of pulsar winds, if they occur at all, most likely occur on time-scales of  $\sim 10^4 - 10^6$  yr.<sup>14,15</sup>

A reasonable alternative is that the pulsar is propagating into a density gradient so that  $\rho$  is increasing as a function of time, causing a decrease in  $r_w$ . However, an increasing density should result in a change in the morphology or surface brightness of the leading edge of G5.27–0.90. In fact, the structure and brightness of the head of G5.27–0.90 is remarkably similar between the two epochs, and also in archival 6 cm VLA data taken at various epochs between 1985 and 1999. There is thus no evidence from the morphology of G5.27–0.90 for a change in ambient conditions between the two epochs.

It thus seems most likely that  $r_w$  has not changed between the two epochs, implying that  $V_p = V_n \ll 1500$  km s<sup>-1</sup>. In this case, demanding that  $t_p \approx \tau$  would mean that the pulsar had only travelled 7' over its lifetime, inconsistent with its separation of 16.1' – 20.6' from the apparent centre of the SNR<sup>8</sup> and thus arguing against a physical association between the two objects. While such chance coincidence along the line-of-sight is not impossible,<sup>16</sup> the strong morphological evidence for an association<sup>5–8,10</sup> leads us to conclude that  $t_p > 39 - 50$  kyr  $\gg \tau$ . This result depends only on assuming that  $V_p = V_n$ , and that the pulsar was born near the SNR’s apparent centre.

Another approach is to let the age of the system, the ambient density and the transverse velocity of the pulsar all be free parameters. We can then solve for these unknowns using the three characteristic length scales of the system,

namely the radius of the SNR ( $R_s = 25d_5$  pc), the stand-off distance of the bow-shock ( $r_w = 0.036d_5$  pc) and the offset of the pulsar from the SNR's centre ( $R_p = [23.4 - 30.0]d_5$  pc). To determine how the unknown quantities relate to  $R_s$ , we first need to determine the SNR's evolutionary state. Using our upper limit  $v_p < 0.59d_5$  and the value measured for  $r_w$ , Equation (1) implies a particle density  $n_1 > n_0 = 0.23\eta d_5^4 \text{ cm}^{-3}$ . Assuming that the SNR is expanding into a similar environment, it will be in the radiative (or ‘‘snowplough’’) phase of its evolution<sup>7,17</sup> if  $t_p > t_R = 13E_{51}^{3/14}n_1^{-4/7}$  kyr, where  $E_{51}10^{51}$  erg is the energy in the supernova explosion and assuming solar ISM abundances. The lower limits we have already computed on  $n_1$  and  $t_p$  ensure that the SNR is indeed in the radiative phase; the radius of the SNR is then given by:<sup>7,17</sup>

$$R_s = 7.0E_{51}^{0.221}n_1^{-0.257}t_3^{0.3} \text{ pc}, \quad (2)$$

where  $t_p = t_3$  kyr. Meanwhile, ballistic motion of the pulsar away from the SNR's centre gives:

$$R_p = 1.02v_p t_3 \text{ pc}, \quad (3)$$

while we can rewrite Equation (1) to show that:

$$r_w = 0.010\eta^{1/2}n_1^{-1/2}v_p^{-1} \text{ pc}. \quad (4)$$

Equations (2), (3) and (4) can be solved simultaneously to give  $v_p = (0.17 - 0.25)E_{51}^{-1.04}\eta^{1.21}d_5^{2.3}$ ,  $n_1 = (1.3 - 2.6)E_{51}^{2.08}\eta^{-1.42}d_5^{-6.6}$  and  $t_3 = (93 - 170)E_{51}^{1.04}\eta^{-1.21}d_5^{-2.3}$ . Self-consistency with the requirement that  $n_1 > n_0$  then implies  $d_5 < 1.3E_{51}^{2.08}\eta^{-2.42}$ , which combined with<sup>8</sup>  $d_5 > 0.9$  (from HI absorption) and  $d_5 \approx 0.9$  (from the pulsar's dispersion measure) justifies the choices  $d_5 = 1$  and  $E_{51} = 1$ .

Thus two different approaches — using either the limits on proper motion, or the morphology of the system — both imply a much older and more slowly moving pulsar than results<sup>6</sup> when one assumes  $t_p = \tau$ . We note that a similar age and velocity to those we have just estimated were derived before the characteristic age of the pulsar was known, by assuming  $n_1 = 1$  and then solving together the equivalents of Equations (2) and (3) (ref. 7).

For a pulsar of constant magnetic dipole moment and moment of inertia, it can be shown that<sup>1</sup>:

$$\frac{t_p}{\tau} = \frac{2}{n-1} \left[ 1 - \left( \frac{\nu}{\nu_0} \right)^{n-1} \right], \quad (5)$$

where  $\nu_0$  is the pulsar's initial rotational frequency and  $n$  is the ‘‘braking index’’, defined by  $\dot{\nu} = -K\nu^n$  (where  $K$  is a constant), and expected to be  $n = 3$  for a dipole rotating *in vacuo*. Our lower limit on  $t_p/\tau$  from proper motion alone implies that  $n < 1.83$ , while the value derived from the morphology of the system argues that  $n < 1.33$ . These values are significantly less than those derived for young pulsars,<sup>18,19</sup> but are similar to  $n = 1.4 \pm 0.2$  observed for the Vela pulsar,<sup>20</sup> a pulsar which also resembles PSR B1757-24 in its value of  $\tau$  and its tendency to glitch.<sup>21</sup> One alternative possibility is that the magnetic field of PSR B1757-24 is growing as a function of time.<sup>22,23</sup> In this case Equation (5) does not hold and  $K$  is no longer a constant;  $\tau$  is then an approximate time-scale for field growth.

Further data can support the conclusion that PSR B1757-24 is much older than  $\tau = \nu/2\dot{\nu}$ : multi-epoch VLBI observations are expected to show westward motion of the pulsar at the level of  $\sim 10$  milliarcsec yr<sup>-1</sup>, X-ray observations of SNR G5.4-1.2 should show emission characteristic of an old rather than young SNR, and a braking index for PSR B1757-24 measured from timing data would be expected to lie in the range predicted above. The low braking

index of the Vela pulsar,<sup>20</sup> discrepant pulsar/SNR ages in other pulsar/SNR associations,<sup>23,24</sup> and the fact that many pulsars with small characteristic ages have no associated SNR,<sup>2,3</sup> all suggest that PSR B1757–24 is not a statistical anomaly. If other pulsars are indeed older than they seem, our understanding of pulsar velocities, asymmetries in supernova explosions, the fraction of supernovae that produce pulsars and the physics of neutron star structure and cooling must all be reconsidered.<sup>12,25–27</sup>

---

Received Accepted .

1. Manchester, R. N. & Taylor, J. H. *Pulsars*. Freeman San Francisco (1977).
2. Braun, R., Goss, W. M. & Lyne, A. G. Three fields containing young pulsars: The observable lifetime of supernova remnants. *Astrophys. J.* **340**, 355–361 (1989).
3. Stappers, B. W., Gaensler, B. M. & Johnston, S. A deep search for pulsar wind nebulae using pulsar gating. *Mon. Not. R. astr. Soc.* **308**, 609–617 (1999).
4. Manchester, R. N., D’Amico, N. & Tuohy, I. R. A search for short period pulsars. *Mon. Not. R. astr. Soc.* **212**, 975–986 (1985).
5. Manchester, R. N., Kaspi, V. M., Johnston, S., Lyne, A. G. & D’Amico, N. A remarkable pulsar–supernova remnant association. *Mon. Not. R. astr. Soc.* **253**, 7P–10P (1991).
6. Frail, D. A. & Kulkarni, S. R. Unusual interaction of the high–velocity pulsar PSR 1757–24 with the supernova remnant G5.4–1.2. *Nature* **352**, 785–787 (1991).
7. Shull, J. M., Fesen, R. A. & Saken, J. M. Pulsar reenergization of old supernova remnant shells. *Astrophys. J.* **346**, 860–868 (1989).
8. Frail, D. A., Kassim, N. E. & Weiler, K. W. Radio imaging of two supernova remnants containing pulsars. *Astron. J.* **107**, 1120–1218 (1994).
9. Becker, R. H. & Helfand, D. J. A new class of nonthermal radio sources. *Nature* **313**, 115–118 (1985).
10. Caswell, J. L., Kesteven, M. J., Komesaroff, M. M., Haynes, R. F., Milne, D. K., Stewart, R. T. & Wilson, S. G. The Galactic radio sources G5.4-1.2 and G5.27-0.90. *Mon. Not. R. astr. Soc.* **225**, 329–334 (1987).
11. Lyne, A. G. & Lorimer, D. R. High birth velocities of radio pulsars. *Nature* **369**, 127–129 (1994).
12. Cordes, J. M. & Chernoff, D. F. Neutron star population dynamics. II. Three-dimensional space velocities of young pulsars. *Astrophys. J.* **505**, 315–338 (1998).
13. van Buren, D. & McCray, R. Bow shocks and bubbles are seen around hot stars by *IRAS*. *Astrophys. J.* **329**, L93–L96 (1988).
14. Frail, D. A. & Scharringhausen, B. R. A radio survey for pulsar wind nebulae. *Astrophys. J.* **480**, 364–370 (1997).
15. Thompson, D. J., Arzoumanian, Z., Bertsch, D. L., Brazier, K. T. S., Chiang, J., D’Amico, N., Dingus, B. L., Esposito, J. A., Fierro, J. M., Fichtel, C. E., Hartman, R. C., Hunter, S. D., Johnston, S., Kanbach, G., Kaspi, V. M., Kniffen, D. A., Lin, Y. C., Lyne, A. G., Manchester, R. N., Mattox, J. R., Mayer-Hasselwander, H. A., Michelson, P. F., Montigny, C. v., Nel, H. I., Nice, D. J., Nolan, P. L., Ramanamurthy, P. V., Shemar, S. L., Schneid, E. J., Sreekumar, P. & Taylor, J. H. EGRET high–energy gamma–ray pulsar studies. I. Young spin–powered pulsars. *Astrophys. J.* **436**, 229–238 (1994).
16. Gaensler, B. M. & Johnston, S. The pulsar / supernova remnant connection. *Mon. Not. R. astr. Soc.* **277**, 1243–1253 (1995).

17. Cioffi, D. F., McKee, C. F. & Bertschinger, E. Dynamics of radiative supernova remnants. *Astrophys. J.* **334**, 252–265 (1988).
18. Lyne, A. G., Pritchard, R. S. & Smith, F. G. Crab pulsar timing 1982–1987. *Mon. Not. R. astr. Soc.* **233**, 667–676 (1988).
19. Kaspi, V. M., Manchester, R. N., Siegman, B., Johnston, S. & Lyne, A. G. On the spin-down of PSR B1509–58. *Astrophys. J.* **422**, L83–L86 (1994).
20. Lyne, A. G., Pritchard, R. S., Graham-Smith, F. & Camilo, F. Very low braking index for the Vela pulsar. *Nature* **381**, 497–498 (1996).
21. Lyne, A. G., Kaspi, V. M., Bailes, M., Manchester, R. N., Taylor, H. & Arzoumanian, Z. A giant glitch in PSR B1757–24. *Mon. Not. R. astr. Soc.* **281**, L14–L16 (1996).
22. Blandford, R. D., Applegate, J. H. & Hernquist, L. Thermal origin of neutron star magnetic fields. *Mon. Not. R. astr. Soc.* **204**, 1025–1048 (1983).
23. Blandford, R. D. & Romani, R. W. On the interpretation of pulsar braking indices. *Mon. Not. R. astr. Soc.* **234**, 57P–60P (1988).
24. Seward, F. D., Harnden Jr., F. R., Murdin, P. & Clark, D. H. MSH 15-52: A supernova remnant containing two compact X-ray sources. *Astrophys. J.* **267**, 698–710 (1983).
25. Frail, D. A., Goss, W. M. & Whiteoak, J. B. Z. The radio lifetime of supernova remnants and the distribution of pulsar velocities at birth. *Astrophys. J.* **437**, 781–793 (1994).
26. Brazier, K. T. S. & Johnston, S. The implications of radio-quiet neutron stars. *Mon. Not. R. astr. Soc.* **305**, 671–679 (1999).
27. Umeda, H., Shibazaki, N., Nomoto, K. & Tsuruta, S. Thermal evolution of neutron stars with internal frictional heating. *Astrophys. J.* **408**, 186–193 (1993).
28. Sault, R. J. & Killeen, N. E. B. *The Miriad User's Guide*. Australia Telescope National Facility Sydney (1998). (<http://www.atnf.csiro.au/computing/software/miriad/>).
29. Keys, R. G. Cubic convolution interpolation for digital image processing. *IEEE Transactions on Acoustics, Speech, and Signal Processing* **29**, 1151–1160 (1981).
30. Powell, M. J. D. A method for minimizing a sum of squares of non-linear functions without calculating derivatives. *The Computer Journal* **7**, 303–307 (1964).

---

## Acknowledgements

We thank Vicky Kaspi and Deepto Chakrabarty for useful discussions, Namir Kassim for supplying 90 cm data on G5.4–1.2 and Andrew Lyne for providing timing data on PSR B1757–24. The National Radio Astronomy Observatory is a facility of the National Science Foundation operated under cooperative agreement by Associated Universities, Inc. B.M.G. acknowledges the support of NASA through a Hubble Fellowship awarded by the Space Telescope Science Institute.

Correspondence should be addressed to B.M.G. (e-mail: [bmg@space.mit.edu](mailto:bmg@space.mit.edu)).

**Table 1.** Very Large Array observations of the pulsar-powered nebula G5.27–0.90 used for proper motion measurements. Both observations used the same pointing centre, namely (J2000) Right Ascension (RA)  $18^{\text{h}}01^{\text{m}}00.035^{\text{s}}$ , Declination (Dec)  $-24^{\circ}51'27.260''$ . Absolute flux densities were determined using observations of the source 3C 286, while antenna gains were calibrated using observations every 15–20 min of the extragalactic source PMN J1751–2524, displaced 2.1 from G5.27–0.90. The resulting images were formed using natural weighting and multi-frequency synthesis with 100 mas pixels, deconvolved using a maximum entropy algorithm, and then smoothed with a circular Gaussian of FWHM  $0''.90$ .

	Epoch 1	Epoch 2
Date Observed	1993 Feb. 02	1999 Oct. 23
Array Configuration	BnA	BnA
On-source integration time (h)	3.3	2.8
Centre Frequency (GHz)	8.44	8.46
Bandwidth (MHz)	75	100

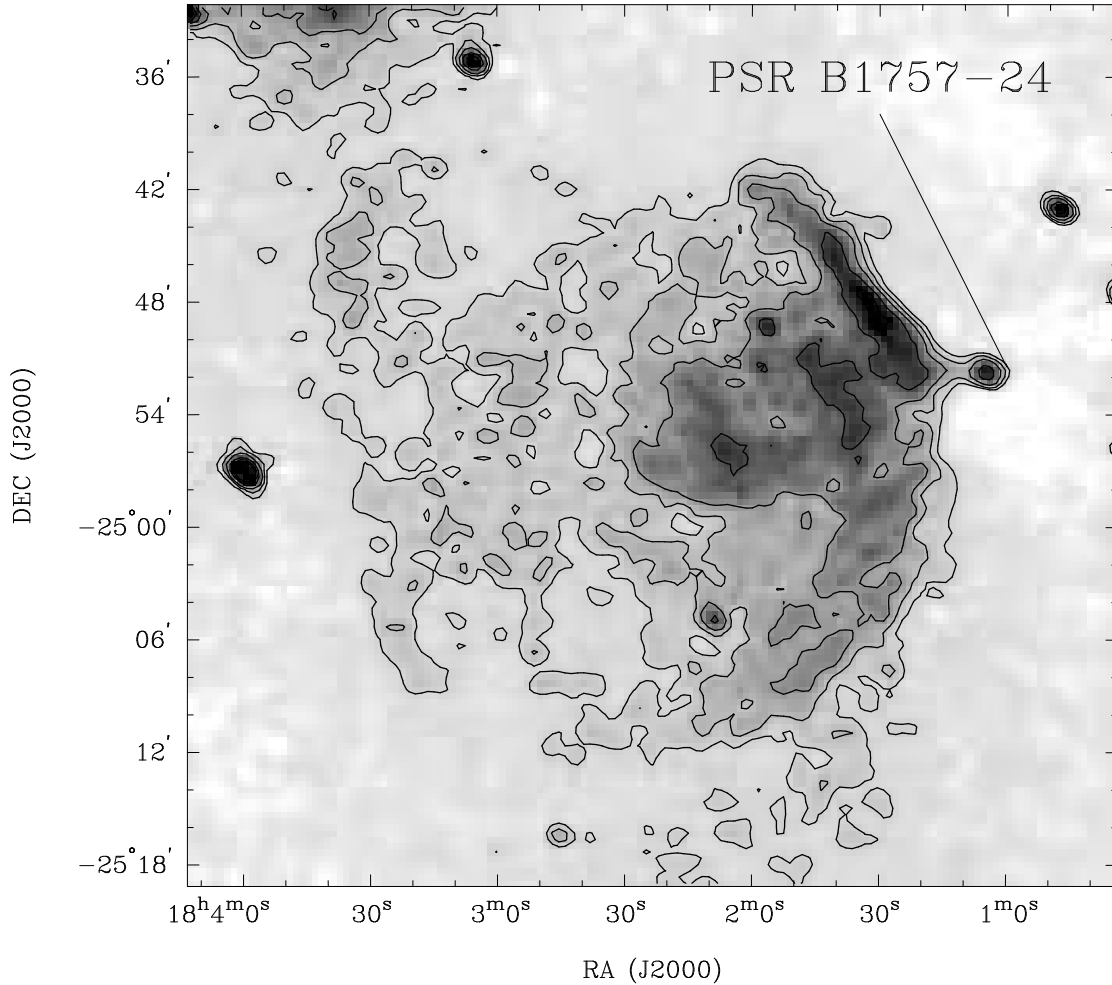


**Figure 1.** Radio emission from the supernova remnant G5.4-1.2. The image corresponds to archival VLA data at an observing wavelength of 90 cm; contours are at levels of 10, 25, 50, 100, 150 and 200  $\text{mJy beam}^{-1}$ , and the peak intensity is  $150 \text{ mJy beam}^{-1}$ . The resolution of the image is  $60'' \times 45''$ . The pulsar (whose position is marked) is at the head of the compact nebula G5.27-0.90 to the west of the supernova remnant.

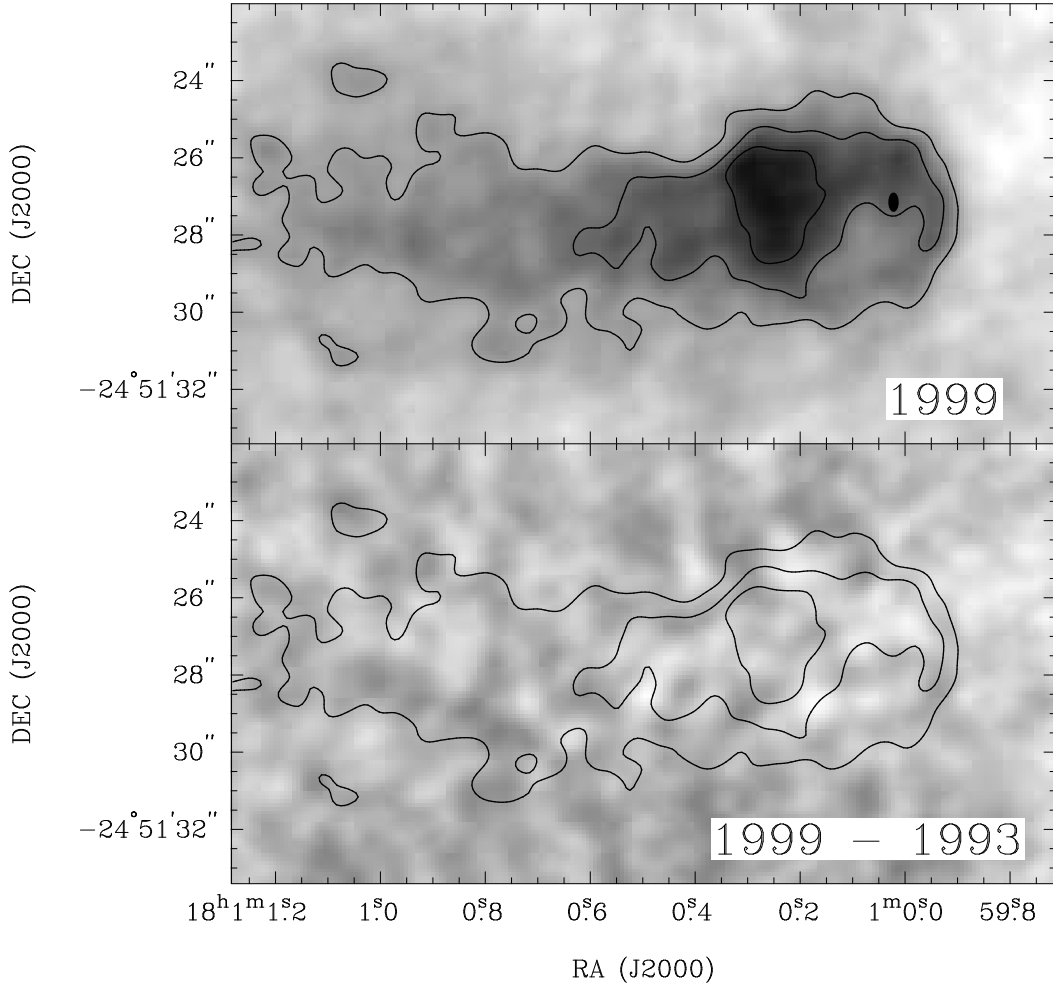


**Figure 2.** Radio emission from the western tip of the pulsar-powered nebula G5.27–0.90. The upper panel represents the 1999 image of G5.27–0.90, with corresponding contour levels at 0.75, 1.5 and 2.25 mJy beam<sup>−1</sup>. The ellipse near the head of the nebula marks the position of PSR B1757–24, (J2000) RA 18<sup>h</sup>01<sup>m</sup>00.023(2)<sup>s</sup>, Dec −24°51′27.15(5)″, which was determined by 20 cm A-array observations in Aug 1999 (uncertainties in the position of the pulsar are a factor of five smaller than the extent of the ellipse). The lower panel shows the difference between the 1999 and 1993 images, on which are superimposed the same contour levels as in the upper panel. To compare the two epochs in a quantitative fashion, we took the deconvolved model from each epoch, computed its two-dimensional Fourier transform, and then sampled this transform with the transfer function corresponding to the  $u - v$  coverage of the 1993 data. Assuming fidelity in the original deconvolution, this results in two data-sets which have identical  $u - v$  coverage and sensitivity, and differ only in the actual brightness distribution between the two epochs. We searched for proper motion between these two images using the MIRIAD task IMDIFF,<sup>28</sup> which finds the shift in  $x$  and  $y$  which minimises<sup>29</sup> the rms noise of the difference map between the two data-sets. Shifts corresponding to a non-integral number of pixels were computed using cubic convolution interpolation.<sup>30</sup> To estimate the uncertainties associated with this approach, we repeated this comparison 40 times, each time adding Gaussian noise of rms 30  $\mu$ Jy beam<sup>−1</sup> (corresponding to the sensitivity of the Epoch 1 data) to one of the images.